



HAL
open science

On the Liquid-Vapor Phase-Change Interface Conditions for Numerical Simulation of Violent Separated Flows

Matthieu Ancellin, Laurent Brosset, Jean-Michel Ghidaglia

► **To cite this version:**

Matthieu Ancellin, Laurent Brosset, Jean-Michel Ghidaglia. On the Liquid-Vapor Phase-Change Interface Conditions for Numerical Simulation of Violent Separated Flows. *Fluid Dynamic and Material Process*, 2020, 16 (2), pp.359-381. 10.32604/fdmp.2020.08642 . hal-04551884

HAL Id: hal-04551884

<https://hal.science/hal-04551884>

Submitted on 6 May 2024

HAL is a multi-disciplinary open access archive for the deposit and dissemination of scientific research documents, whether they are published or not. The documents may come from teaching and research institutions in France or abroad, or from public or private research centers.

L'archive ouverte pluridisciplinaire **HAL**, est destinée au dépôt et à la diffusion de documents scientifiques de niveau recherche, publiés ou non, émanant des établissements d'enseignement et de recherche français ou étrangers, des laboratoires publics ou privés.

On the Liquid-Vapor Phase-Change Interface Conditions for Numerical Simulation of Violent Separated Flows

Matthieu Ancellin^{1, *}, Laurent Brosset² and Jean-Michel Ghidaglia¹

Abstract: Numerous models have been proposed in the literature to include phase change into numerical simulations of two-phase flows. This review paper presents the modeling options that have been taken in order to obtain a model for violent separated flows with application to sloshing wave impacts. A relaxation model based on linear non-equilibrium thermodynamics has been chosen to compute the rate of phase change. The integration in the system of partial differential equations is done through a non-conservative advection term. For each of these modelling choices, some alternative models from the literature are presented and discussed. The theoretical framework for all phase change model (conservation equations and entropy growth) is also summarized.

Keywords: Phase change modeling, two-phase flow, non-equilibrium thermodynamics, compressible flow, hyperbolic system of conservation laws.

1 Introduction

Evaporation and condensation play an important role in many natural and industrial processes. In particular, the motivation of the present work is the study of wave impacts in cryogenic tanks in which the fluid is at equilibrium with its vapor phase [Ancellin (2017); Ancellin, Brosset and Ghidaglia (2018c)]. This phenomenon is brief and violent: its modeling requires the use of two compressible fluids without thermodynamical equilibrium hypothesis.

Other examples of violent flows with phase change can be found in the literature, such as the damping of explosions in aqueous foams [Faure and Ghidaglia (2011)] or the steam explosions in nuclear power plants [Berthoud (2000)]. However, these two examples require models on a different scale than the wave impact problem.

¹ Université Paris-Saclay, ENS Paris-Saclay, CNRS, Centre Borelli, Gif-sur-Yvette, France.

² GTT (Gaztransport & Technigaz), Saint-Rémy-lès-Chevreuse, France.

* Corresponding Author: Matthieu Ancellin. Email: matthieu.ancellin@ens-paris-saclay.fr.

Received: 24 September 2019; Accepted: 03 March 2020.

Indeed, considering only continuum mechanics, the representations of the interface in two-phase models can be roughly grouped in three different categories depending of the scale of the problem:

Thick interface: At the smallest scales, the interface can be seen as a thick layer in which the physical properties vary continuously between liquid and gas. In Jamet et al. [Jamet, Lebaigue, Coutris et al. (2001)] a phase-field-like model for two compressible fluid with phase-change is presented.

DNS scale: At a large scale with respect to the thickness of the interface the interface can be seen as a sharp discontinuity between two separated pure phases. Following [Tryggvason, Scardovelli and Zaleski (2011)], this category of model can be denoted as the “Direct Numerical Simulation” (DNS) scale, in contrast with the next category. Examples of such models include [Juric and Tryggvason (1998); Welch and Wilson (2000)] for incompressible flows with phase change using respectively an interface tracking method and a Volume-of-Fluid (VOF) method. Other examples (including compressible flow) are discussed later in the paper.

Averaged field: At an even larger scale or for turbulent flows, the shape of the interface might become complex, its exact tracking (analytically or numerically) might become difficult and/or irrelevant. Instead, only the averaged information can be modeled. Baer et al. [Baer and Nunziato (1986)] and their followers [Kapila, Menikoff, Bdzil et al. (2001)] discuss the modeling of granular materials and have been seminal in the field of average-field models. Bestion [Bestion (1990)] presents such a model for liquid-vapor flow with phase change in an industrial simulation code. Ishii et al. [Ishii and Hibiki (2011)] provide a complete derivation of an average-field model for multi-phase flow. As examples of more recent works with phase change, we can cite [Chiapolino, Boivin and Saurel (2017); De Lorenzo, Lafon and Pelanti (2019)].

Each of the categories above is the limit of the previous one when the spatial scale of the problem increases. In general, it is difficult to assign a precise length scale to each category, since it depends on many parameters, such as the properties of the fluid (in particular the surface tension) or the environmental pressure and temperature conditions. The computational power available for numerical simulations might also affect the choice of the model. As an example, some estimates can be given for water and air in usual conditions: the thick interface models are relevant for characteristic lengths below a micrometer, whereas the average-field models are rarely used below several centimeters.

At each time when passing from a model to a higher scale model, a closure relation should be used to define the physics of the lower scale. For instance, the capillary force at the thick-interface scale will appear at the DNS scale under the form of surface tension at the interface. At the averaged-field scale, it will influence the size and shape of bubbles and droplets and thus the closure equations needed to model the behavior of the fluid.

In a similar way, phase change appears under different forms at the different scales.

Note that problems involving different physics may involve several different scales at once. For instance Baer et al. [Baer and Nunziato (1986)] describes the behavior of a flame front, represented as a thick interface, between two mixtures of gas and granular material, represented with averaged fields.

The distinction between the different scales can become blurrier when the numerical resolution of the model is considered. Indeed, some DNS scale models introduce a numerical mixture zone at the interface in order to ease the numerical capture of the interface. Despite the similarity of such a numerical model with the thick-interface scale and the average-field scale, they should not be confused. In particular, one should keep in mind that this numerical diffuse interface is only a numerical artifact and its influence on the results should be as low as possible.

In the present paper, we discuss the modeling of phase change at the DNS scale. More precisely, the following hypotheses are made:

1. The interface is a sharp discontinuity between two pure immiscible fluids, as represented on Fig. 1.
2. The two phases can be described by any equation of state as long as the phases are qualitatively distinguishable. This means in particular that no super-critical fluids can be considered. This hypothesis is actually deeply related to the previous one: close to the critical point, the thickness of the interface is expected to be larger [Jamet, Lebaigue, Coutris et al. (2001)] and the previous hypothesis would not hold anymore.

Even if we do not model the evolution of the system near the critical point, cubic equations of state (such as the van-der-Walls equation of state) could be used, once they have been restricted to a domain far from the critical point. The two branches of the EOS corresponding to the two different phases would be considered as two distinct equations of states.

The inability to model super-critical fluids is a limitation of the present work. But the use of two equations of state makes the present work easily portable to other problem of interfacial mass exchange (such as liquid-solid phase-change), which would not be the case of a single cubic equation of state.

Although in practice simple analytical equations of state (such as the ideal gas or stiffened gas equations of state) are used most of the time, the same approach is applicable to any equation of state, including tabulated ones (for example, the tabulated equations of state for water and methane presented in Labourdette et al. [Labourdette, Ghidaglia, Redford et al. (2017)]).

3. The pure phases might go out of their thermodynamical stability region and exist as metastable phases. The creation of new interfaces by nucleation when the fluid is out of equilibrium will not be considered. The spinodal point, beyond which the fluids cannot be metastable anymore, will also be ignored. In other words, the phases are metastable in their whole non-stability domain.
4. Both liquid and gas will be seen as compressible.
5. Finally, surface tension, viscosity and turbulence are out of the scope of the present paper.

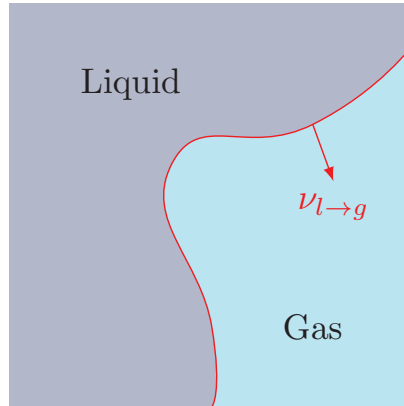


Figure 1: Scheme of two pure phases separated by a smooth interface (with $v_{l \rightarrow g}$ the normal oriented from the liquid side to the gas side)

The paper is organized in three parts corresponding to different stages of the development of a simulation code. Firstly, the local conditions at the interface are discussed. Then the interface boundary conditions are included into a system of partial differential equations modeling the two-phase flow. Finally, the discretization of this system is briefly discussed. This last part is kept short, since more extended presentations can be found in other papers [Ancellin, Brosset and Ghidaglia (2018b, 2019)]. In each section of the paper, some modeling decisions have to be made. Pros and cons of the chosen approach are discussed.

The discussion is only based on theoretical and numerical arguments. Data from experiments would be necessary to close the model and validate the results. This is out of the scope of the present work in which we only present a modeling strategy based on the fundamentals of phase change and discuss how to include it robustly into a two-fluid code.

This paper is part of a series of work on the influence of phase change on wave impact loads. Parts of the present paper have already been published in French in Ancellin [Ancellin (2017)]. The numerical simulation of two-phase flows with phase change is also discussed in Ancellin et al. [Ancellin, Brosset and Ghidaglia (2018b, 2019)]. Physical conclusions can be found in Ancellin et al. [Ancellin, Brosset and Ghidaglia (2018c)].

2 Modeling the interface with phase change

2.1 Rankine-Hugoniot conditions

Let us consider an interface between two phases (see Fig. 1), through which there is a mass flow. We denote by $\llbracket X \rrbracket$ the jump of the magnitude X across the interface. That is $\llbracket X \rrbracket = X_l - X_g$ where the g and l subscripts denote respectively the state on the gas and liquid side of the interface.

The conservation of mass, momentum and energy can be written in the reference frame of the interface as:

$$\llbracket \rho u \rrbracket \cdot v_{l \rightarrow g} = 0, \quad (1)$$

$$\llbracket \rho u \otimes u + p \mathbb{I} \rrbracket v_{l \rightarrow g} = 0, \quad (2)$$

$$\llbracket \rho \left(e + \frac{|u|^2}{2} \right) u + pu + q \rrbracket \cdot v_{l \rightarrow g} = 0, \quad (3)$$

where $v_{l \rightarrow g}$ is the normal vector at the interface oriented from the liquid side to the gas side, ρ is the density, u the velocity in the reference frame of the interface, p the pressure, e the specific internal energy and q the heat diffusion flux.

Let us define the mass flow rate across the interface $J_{l \rightarrow g}$ (counted positively for evaporation) using Eq. (1):

$$J_{l \rightarrow g} := \rho_g u_g \cdot v_{l \rightarrow g} = \rho_l u_l \cdot v_{l \rightarrow g}. \quad (4)$$

With this notation, the Eqs. (2) and (3) can be rewritten as follow (see [Delhay (1974); Ancellin (2017)]).

$$\llbracket p \rrbracket + J_{l \rightarrow g}^2 \llbracket \tau \rrbracket = 0, \quad J_{l \rightarrow g} \llbracket u \rrbracket \cdot t = 0 \quad (5)$$

$$J_{l \rightarrow g} \llbracket h \rrbracket + \frac{J_{l \rightarrow g}^3}{2} \llbracket \tau^2 \rrbracket = \llbracket q \rrbracket \cdot v_{l \rightarrow g}, \quad (6)$$

where t is any tangential vector at the interface and $\tau = \frac{1}{\rho}$ is the specific volume.

The pressure jump in the first part of Eq. (5) can be seen as a Venturi effect at the interface. The second part of Eq. (5) imposes the continuity of the tangential velocity at the interface, even without viscosity. The release or capture of latent heat is implicit in Eq. (6). By definition of the latent heat, the equation of states of the phases are such that at any temperature T :

$$\llbracket h(p^{\text{sat}}(T), T) \rrbracket = \mathcal{L}(T) \quad (7)$$

where h is the specific enthalpy and \mathcal{L} is the latent heat of the chemical species at temperature T .

The second term of Eq. (6) is the contribution of the kinetic energy to the energy balance. In general, it is small with respect to the latent heat in the first term and can be neglected in first approximation.

The above relationships are not specific to phase change but can describe any permeable interface between two fluids. For instance, they can describe the flame front in some model for combustion: the two fluids are then unburnt gas and burnt gas. They are the same as the Rankine-Hugoniot relations around a shock wave [Menikoff and Plohr (1989)], except for the heat diffusion term in the energy balance. See Appendix A for an example of Hugoniot diagrams in the case of phase change.

For phase change this heat diffusion term cannot be neglected: without it, Eq. (6) can be approximated as $[[h]] = 0$ which, for realistic equations of state including latent heat, would lead to temperature jumps of several hundreds of Kelvin across the interface. Modeling a liquid-vapor interface without heat exchanges makes no sense from the point of view of physics. This fact is also discussed in Fechter et al. [Fechter, Munz, Rohde et al. (2017)].

Thein [Thein (2018)] also invokes another argument to state that adiabatic phase change is unphysical, which is the stability of the adiabatic compression: many usual gases would not condensate when compressed adiabatically. However, this other phenomenon only concerns the nucleation in pure phase and not the behavior of an existing interface which is the topic of the present paper.

In the next sections, it will be convenient to see the interface as a shock. However, one should keep in mind that this shock is tightly coupled with the heat conduction which has to be modeled along.

2.2 Closure relations

Two closure equations are missing from the above boundary conditions, for the mass and heat flux across the interface. Let us assume that the mass and heat flux at the interface can be written as functions of the local thermodynamical conditions near the interface:

$$J = \mathcal{J}(p_g, T_g, p_l, T_l), \quad Q = \mathcal{Q}(p_g, T_g, p_l, T_l). \quad (8)$$

These two relations might be called a “kinetic relation” in reference to the kinetic relations found in other works. Abeyaratne et al. [Abeyaratne and Knowles (1991)] introduce a kinetic relation to the model the evolution of phase boundaries in solids. Merkle et al. [Merkle and Rohde (2007)] and Thein [Thein (2018)] use a similar formalism for phase change between liquid and gas. The choice of \mathcal{J} and \mathcal{Q} is an open problem. Some possible models will be discussed in this section.

The fact that we can define pressure and temperatures on both sides of the interface depends on some local thermodynamical equilibrium. Only the assumption of a non-equilibrium between the two sides of the interface is made.

Without phase change ($J=0$), the closure relation on Q could be chosen as

$$Q_{l \rightarrow g} = q_l \cdot v_{l \rightarrow g} = q_g \cdot v_{l \rightarrow g} = \frac{k_{\text{int}}}{\epsilon} (T_l - T_g), \quad (9)$$

where k_{int} is the mean thermal conductivity in a boundary layer of thickness ϵ . The classical hypothesis of a continuous temperature at the interface can be found when $\epsilon \rightarrow 0$.

Similarly, the mass exchange term can be written as a relaxation process. Such a relaxation can be derived in the framework of *linear non-equilibrium thermodynamics* [Bedeaux, Hermans and Ytrehus (1990); Bedeaux and Kjelstrup (2004)]. In this framework, a flux is written as a function of the nonequilibrium that drives it:

$$\text{Flux} = f(\text{nonequilibrium}),$$

with $f(0)=0$, since there should be no flux when the system is at equilibrium. Assuming small non-equilibrium, the function can be linearized:

Flux = constant \times nonequilibrium.

The modeling requires then the identification of the flux and nonequilibrium of the system, as well as the evaluation of the constant relating them. This is usually done using the entropy growth rate, in order to ensure that the model complies with the Second Principle of Thermodynamics.

For the interface with phase change, the entropy balance can be written as [Delhaye (1974); Ancellin (2017)]

$$J_{l \rightarrow g}[s] + \left[\frac{q}{T} \right] \cdot v_{l \rightarrow g} \geq 0, \quad (10)$$

where s is the specific entropy of the fluid.

There are still infinitely many possible closure relations respecting this entropy growth condition. To choose one in particular, some assumptions have to be made, based on physical considerations. After some approximations [Ancellin (2017)], the entropy balance can be rewritten as

$$- J_{l \rightarrow g} \frac{\mu_g(p_g, T_l) - \mu_l(p_g, T_l)}{T_l} + (Q_{l \rightarrow g} - J_{l \rightarrow g} h_g(T_g)) \left(\frac{1}{T_g} - \frac{1}{T_l} \right) \geq 0, \quad (11)$$

where μ is the chemical potential (which is equal to the specific free enthalpy, since we are studying pure phases) and $Q_{l \rightarrow g}$ is the energy flow rate defined by Eq. (6):

$$\begin{aligned} Q_{l \rightarrow g} &= J_{l \rightarrow g} \left(h_g + \frac{|u_g|^2}{2} \right) + q_g \cdot v_{l \rightarrow g}, \\ &= J_{l \rightarrow g} \left(h_l + \frac{|u_l|^2}{2} \right) + q_l \cdot v_{l \rightarrow g}. \end{aligned} \quad (12)$$

From Eq. (11), the following kinetic relations can be shown to be compatible with the second principle of thermodynamics:

$$Q_{l \rightarrow g} = G_q (T_l - T_g) + h_g(p_g, T_g) J_{l \rightarrow g}, \quad J_{l \rightarrow g} = G_m \frac{\mu_l(p_l, T_l) - \mu_g(p_g, T_l)}{T_l}, \quad (13)$$

where G_m and G_q are (positive) relaxation rates.

The above equation for the mass flux can be linearized to retrieve a relation similar to the common Hertz-Knudsen relation:

$$\begin{aligned}
 Q_{l \rightarrow g} &= G_q (T_l - T_g) + h_g(p_g, T_g) J_{l \rightarrow g}, \\
 J_{l \rightarrow g} &= -G_m \frac{\tau_g(p^{\text{sat}}(T_l), T_l)}{T_l} (p_g - p^{\text{sat}}(T_l)).
 \end{aligned} \tag{14}$$

We refer the reader to Bond et al. [Bond and Struchtrup (2004)] and Badam et al. [Badam, Kumar, Durst et al. (2007)] for an overview of some models of nonequilibrium phase change, including the Hertz-Knudsen model.

On Fig. 2, the values of the mass flow rate of the expressions Eqs. (13) and (14) are compared. As expected, both expressions are zero on the saturation curve. Near the saturation curve, the two surfaces are tangent. Further from the saturation curve, the mass flow rates predicted by the two expressions can be quite different.

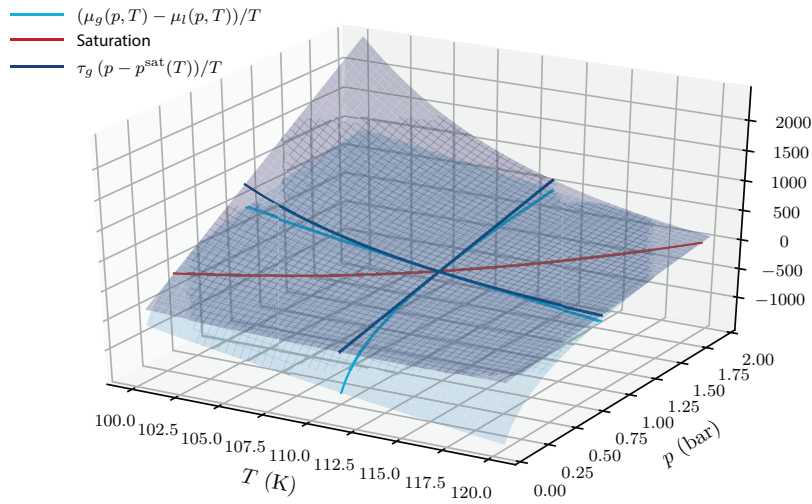


Figure 2: Mass flow rate (counted positively for condensation) predicted by the expressions Eqs. (13) and (14) for pressures $p_g = p_l = p$ between 0.1 bar and 2 bar and temperatures $T_g = T_l = T$ between 100 K and 120 K. The red line is the saturation curve $p = p^{\text{sat}}(T)$, at which the mass flow rate is zero

However, linear non-equilibrium thermodynamics makes the hypothesis of a small distance to equilibrium. In particular, the linear expression derived above are not compatible with the existence of a maximal Chapman-Jouguet mass flow rate (see Appendix A). The modification of the Hertz-Knudsen equation by Schrage [Schrage (1953)] might be seen as a way to incorporate this upper bound. Alternatively, some works suggest to use the rate of the Chapman-Jouguet point as a closure relation instead of the relaxation expressions (see [Le Métayer, Massoni and Saurel (2005); Perrier (2008)]).

Note that the saturation curve (p^{sat}) appearing in the expression above is not part of the closure relation itself, but is actually fully determined by the full equations of states of the two-fluids (see [Le Métayer, Massoni and Saurel (2004)] for the fit of a full analytical equation of state, including the saturation curve, on experimental data and Krafcik et al. [Krafcik and Velasco (2014)] for a discussion of the approximation of the saturation curve at first-order (Clausius-Clapeyron formula) and higher order).

For slow problems, the hypothesis of an instantaneous relaxation to equilibrium can be made. Formally, this can be seen as setting $G \rightarrow \infty$. For the heat flux, this leads to the temperature continuity condition $T_g = T_l$. For the phase change mass flow rate, the equilibrium condition $p = p^{\text{sat}}(T)$ holds at all time and the mass flow rate $J_{l \rightarrow g}$ can be seen as a Lagrange multiplier ensuring this equilibrium condition. However, most implementations of the equilibrium model do not use the formalism of a Lagrange multiplier (except for instance [Martin, Chaouki, Robert et al. (2016)]). They instead follow the strategy of the Stefan problem [Stefan (1890)] and compute the mass flow rate from the energy balance Eq. (6) (see [Juric and Tryggvason (1998); Sato and Ničeno (2013)] for two examples of interface tracking methods with equilibrium phase change at the interface).

3 Inclusion in a two-fluid model

In the previous section, the local conditions near the interface have been discussed. In the present section, the goal is the embedding of these local boundary conditions into a global model of the flow, that is the two-fluid Euler equations.

Intrinsically, the phase change boundary conditions are boundary conditions and could be treated as such. The Stephan phase change problem [Stefan (1890)] has become in mathematics a reference toy model of a PDE on two domains with a moving boundary condition in between. Interface tracking [Juric and Tryggvason (1998)] or Lagrangian methods allow to keep track of two separated domain and to impose a boundary condition at the interface.

Instead, in the present paper, we focus on “single domain” representation of the two-phase flow (also called sometimes “single fluid” approach). The two fluid will be identified by a characteristic function χ with value $\chi=0$ in the liquid and $\chi=1$ in the gas. The Euler conservation equations reads

$$\begin{aligned} \partial_t \rho + \nabla \cdot (\rho u) &= 0, \\ \partial_t (\rho u) + \nabla \cdot (\rho u \otimes u + p \mathbb{I}) &= 0, \\ \partial_t (\rho E) + \nabla \cdot ((\rho E + p)u + q) &= 0, \end{aligned} \tag{15}$$

where $E = e + \frac{|u|^2}{2}$ is the specific total energy. An evolution equation for χ needs to be added to complete the system (and implicitly to describe the evolution of the interface between the $\chi=0$ region and the $\chi=1$ region). Without phase change, it can take the form of a conservation equation for the mass of gas:

$$\partial_t(\rho\chi) + \nabla \cdot (\rho\chi u) = 0 \quad (16)$$

The whole domain can be seen as a single fluid with an equation of state of the following form:

$$\rho(p, T, \chi) = \begin{cases} \rho_l(p, T) & \text{if } \chi = 0, \\ \rho_g(p, T) & \text{if } \chi = 1, \end{cases} \quad e(p, T, \chi) = \begin{cases} e_l(p, T) & \text{if } \chi = 0, \\ e_g(p, T) & \text{if } \chi = 1, \end{cases} \quad (17)$$

where ρ_l, e_l are the density and specific internal energy of the liquid and ρ_g, e_g are the density and specific internal energy of the gas.

The two fluids with two equations of state ρ_l, e_l and ρ_g, e_g are represented here as a single fluid with an order parameter χ . Since we made the hypothesis that the two fluids are separated, values of χ other than 0 and 1 do not have any physical sense. The handling of the discontinuity of χ at the interface might be a difficulty for the numerical resolution. To make the simulation easier, a locally averaged model might be derived from the above equation. A mixture model (that is an extension of Eq. (17) for $0 < \chi < 1$) would need to be introduced to describe the behavior of mixed areas [Ancellin, Brosset and Ghidaglia (2018b)]. However, the mixture law will then be a bias of the numerical resolution, not a part of the physical problem, which only involves separated phases.

To complete the PDE, boundary conditions have to be defined. They are out of the scope of the present paper. The description of the contact point between the liquid-vapor interface and a wall might be a difficult problem, and for the sake of simplicity will not be discussed here.

3.1 Strategies to include phase change term

The inclusion of phase change in a single-domain model (with a numerical mixture layer at the interface or not) can take several forms. We can roughly sort them into two main categories with each two sub-categories, depending on the way in which the phase change term appears in the PDE:

3.1.1 Diffuse volumic term (terms of order zero in the PDE)

At the interface: When the interface has been averaged, a mass exchange term of order zero can be added in the mixture cells near the interface (see e.g., [Le Martelot, Saurel and Nkonga (2014); Saurel, Petitpas and Abgrall (2008); Saurel, Boivin and Le Métayer (2016)] for compressible flows or Wang et al. [Wang, Dong and Zhan (2017)] for an exemple of incompressible flow). The gas mass conservation Eq. (16) then takes the form:

$$\partial_t(\rho\chi) + \nabla \cdot (\rho\chi u) = \mathcal{A}J_{l \rightarrow g} \quad (18)$$

where \mathcal{A} is a coefficient estimating the local interfacial area. This approach allows to use the same model as for higher scale average-field models. The motion of the interface due to phase change can then be seen as a front propagation in a reaction-diffusion problem. However, it is not easy to ensure that this kind of front propagation converges to the desired sharp front when the width of the interface goes to zero. The limit of reaction-diffusion models when the thickness of the interface goes to zero is discussed for instance in Witterstein et al. [Witterstein (2010); Alt and Witterstein (2011)].

Away from the interface: Another strategy has been proposed by Hardt et al. [Hardt and Wondra (2008)]. In order to simplify the numerical handling of the interface, volumic mass sources and sinks are distributed a few cells away from the interface. Phase change is thus a non-local effect of mass disappearing in a pure phase and reappearing a couple of cells away on the other side of the interface. It might help the implementation of phase change in existing interface model, but should be done with care: if the phase change is applied far from the interface, the local properties used to compute the mass flow rate also have to be computed on a larger stencil.

3.1.2 Captured shock-like interface

In the previous section of this paper, we discussed how the boundary conditions at the liquid-vapor interface are similar to the boundary conditions of a shock-wave.

Considering the interface as a shock has several advantages. The main one is that the mass flow rate can then be included in the resolution of the Riemann problem in an (approximate) Riemann solver (see Fig. 3). In this way, the compression or expansion of the fluid that is required to accommodate the change of density can be directly coupled to the phase change rate.

Two approaches can be used to include this shock in the solution of the Riemann problem:

With ad-hoc solutions to the Riemann problem: The wave corresponding to the liquid-vapor interface in the solution of the Riemann problem can be adapted to match the phase-change boundary conditions. This method has been studied in a series of works such as [Godlewski and Seguin (2006); Rohde and Zeiler (2015); Thein (2018)]. Most of them are based on a cubic equation of states and do not use a characteristic function χ to distinguish the phases as discussed above. The “ad-hoc Riemann solver” is a weak solution for the Euler equations with this equation of state including a non-classical phase change shock wave.

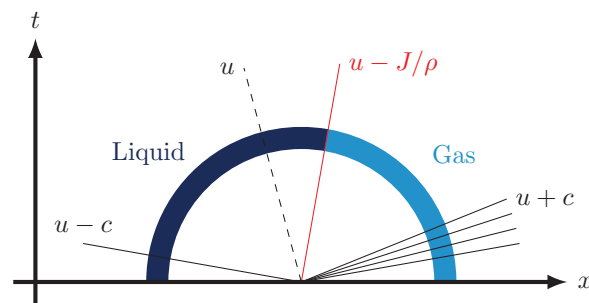


Figure 3: Example of the solution of a Riemann problem with an interface with condensation. The phase change interface evolves with a velocity different from the contact discontinuity of velocity u . The liquid in between the two waves is the newly condensed liquid. Because of the ratio of density between the two phases, the pressure is reduced, which influences the behavior of the two sonic waves with velocities $u-c$ and $u+c$. See also [Ancellin (2017); Ancellin, Brosset and Ghidaglia (2018a)]

With an interface advection term: The method followed by the authors of the present paper is based on the advection equation that the interface should follow:

$$\partial_t \chi + \left(u - \frac{J}{\rho} \right) \cdot \nabla \chi = 0, \quad (19)$$

which can be combined with the Euler conservation equations to give the following gas mass balance equation:

$$\partial_t(\rho\chi) + \nabla \cdot (\rho\chi u) - J \cdot \nabla \chi = 0. \quad (20)$$

It can be seen as a variant of the ad-hoc Riemann solver. Indeed, the solution of the Riemann problem for the system Eqs. (15) and (20) is similar to the solution of the ad-hoc Riemann solver. With this approach, the boundary conditions at the liquid-vapor interface do not need to be explicitly written but appear implicitly from Eq. (15) and from the expression of J used in Eq. (20).

In Eq. (20), $J \cdot \nabla \chi > 0$ corresponds to evaporation (the mass of gas is increasing) and $J \cdot \nabla \chi < 0$ corresponds to condensation (the mass of gas is decreasing). This approach can be seen a special case of Eq. (18), where the interfacial area density is replaced by $\nabla \chi$ which is non-zero only at the interface. It seems to us to be a more accurate approach that taking $\mathcal{A} \rightarrow \infty$ at the sharp interface as suggested by Saurel et al. [Saurel, Boivin and Le Métayer (2016)].

Finally, the full system we consider reads:

$$\begin{aligned} \partial_t \rho + \nabla \cdot (\rho u) &= 0, \\ \partial_t(\rho u) + \nabla \cdot (\rho u \otimes u + p \mathbb{I}) &= 0, \\ \partial_t(\rho E) + \nabla \cdot ((\rho E + p)u + q) &= 0, \\ \partial_t(\rho\chi) + \nabla \cdot (\rho\chi u) - J \cdot \nabla \chi &= 0, \end{aligned} \quad (21)$$

with an equation of state of the form Eq. (17) and a closure relation on J (see also Appendix B).

3.2 Discussion of the conservation equations and other expressions

The system Eq. (21) is sufficient to describe the physics of the two-phase flow with phase change. In the present section, some other expressions are derived in order to put the emphasis on some particular aspects of this model.

In Eq. (21) the equations of conservation of total mass, total momentum and total energy are unaffected by the introduction of the phase change term. Indeed, phase change does not break the principle of conservation of total mass, total momentum and total energy. However, phase change is an exchange between the two phases: when we derive balance laws for the mass of gas (resp. liquid), the momentum of the gas (resp. liquid) and the energy of the gas (resp. liquid), then exchange terms appear.

The Eq. (19) has been combined with the total mass conservation equation to get the Eq. (20) which is the balance law for the mass of gas. The same can be done with the

conservation of total momentum and total energy. Thus, the following balance laws for the mass, momentum and energy of each individual species can be obtained:

$$\begin{aligned}
 \partial_t(\chi\rho) + \nabla \cdot (\chi\rho u) - J \cdot \nabla\chi &= 0, \\
 \partial_t(\chi\rho u) + \nabla \cdot \chi(\rho u \otimes u + p\mathbb{I}) - (u \otimes J + p\mathbb{I})\nabla\chi &= 0, \\
 \partial_t(\chi\rho E) + \nabla \cdot \chi((\rho E + p)u + q) - (JE + pu + q) \cdot \nabla\chi &= 0, \\
 \partial_t((1 - \chi)\rho) + \nabla \cdot (1 - \chi)\rho u + J \cdot \nabla\chi &= 0, \\
 \partial_t((1 - \chi)\rho u) + \nabla \cdot (1 - \chi)(\rho u \otimes u + p\mathbb{I}) + (u \otimes J + p\mathbb{I})\nabla\chi &= 0, \\
 \partial_t((1 - \chi)\rho E) + \nabla \cdot (1 - \chi)((\rho E + p)u + q) + (JE + pu + q) \cdot \nabla\chi &= 0,
 \end{aligned} \tag{22}$$

The terms on the right involving $\nabla\chi$ are the exchanges between the two phases. Among them, the terms containing the mass flow rate J are the exchanges of mass, momentum and energy between phases due to phase change (or more precisely, the momentum and the energy carried from one phase to the other by the exchanged mass). The terms $p\nabla\chi$ in the momentum equations and its counterpart in the energy equation are the mechanical exchange of momentum between the phases due to pression.

The reader might expect the latent heat to appear as a source term in the energy balance. In the rest of this section, such a source is derived from the expressions above. For the sake of simplicity, let us neglect the kinetic energy and the work of the pressure force. The energy conservation equation from Eq. (21) will be approximated as an advection equation for the specific enthalpy:

$$\partial_t h + u \cdot \nabla h + \nabla q = 0, \tag{23}$$

where the enthalpy h is defined as in Eq. (17) as

$$h(p, T, \chi) = \begin{cases} h_l(p, T) & \text{if } \chi = 0, \\ h_g(p, T) & \text{if } \chi = 1, \end{cases}$$

that is

$$h(p, T, \chi) = \chi h_g(p, T) + (1 - \chi) h_l(p, T). \tag{24}$$

Moreover, let us assume the following classical linearization of h_g and h_l :

$$h_g(p, T) = C_{pg}(T - T_0) + \mathcal{L}(T_0), \quad h_l(p, T) = C_{pl}(T - T_0), \tag{25}$$

where T is the temperature, T_0 is a given reference temperature, C_{pg} and C_{pl} are the heat capacities of the gas and the liquid at T_0 , and \mathcal{L} is the specific latent heat at T_0 which by definition follows $\mathcal{L}(T_0) = h_g(T_0) - h_l(T_0)$. Then Eq. (24) can be rewritten as

$$h(p, T, \chi) = C_p(T - T_0) + \chi\mathcal{L}(T_0), \tag{26}$$

where $C_p = \chi C_{pg} + (1 - \chi) C_{pl}$ is the heat capacity of the “single fluid”.

The evolution Eq. (23) can then be rewritten as:

$$\partial_t(C_p T) + u \cdot \nabla(C_p T) + \nabla q = -\mathcal{L}(T_0) \frac{J}{\rho} \cdot \nabla \chi, \quad (27)$$

When $J \cdot \nabla \chi < 0$, the fluid is condensating, latent heat is released and the right-hand-side acts as a source term for the thermal energy $C_p T$. This form of phase change modelling is more common in many models, such as for instance [Arid, Kousksou, Jegadheeswaran et al. (2012)].

4 Numerical resolution

Two approaches for the discretization of the interface advection term have been presented in Ancellin et al. [Ancellin, Brosset and Ghidaglia (2018b, 2019)]. Let us briefly summarize them.

In Ancellin et al. [Ancellin, Brosset and Ghidaglia (2018b)], the interface is represented in the code by a VOF-type method without reconstruction of the interface. The evolution equations are locally averaged in order to obtain evolution equations for the mixed cells. The nonconservative term corresponding to the average version of the interface advection term is locally linearized at each interface in order to obtain a hyperbolic system of conservation equations. This set of equation is discretized with a Roe-type approximate Riemann solver [Ghidaglia, Kumbaro and Le Coq (2001)].

This approach has two limitations: firstly, due to the numerical diffusion of the scheme, the number of mixed cells near the interface can increase, thus reducing the accuracy of the result; secondly, a rigorous and robust handling of the latent heat in the mixed cell is not easy and only an isothermal model has been presented in Ancellin et al. [Ancellin, Brosset and Ghidaglia (2018b)].

These two limitations have been circumvented in Ancellin et al. [Ancellin, Brosset and Ghidaglia (2019)] by using the interface reconstruction scheme introduced by Braeunig [Braeunig (2007)]. No mixed cell, nor averaged form of the equation is required anymore. The advection of the reconstructed interface is done in a Lagrangian formalism, using the same approximate Riemann solver. The heat diffusion is solved separately using a time splitting approach.

The decision to solve separately the heat diffusion from phase change was risky: both are closely coupled and using only a weak coupling may lead to a less robust code. Still, the time splitting approach is working fine at least for small time steps and moderate phase change mass flow rate.

On the other hand, phase change also needs to be coupled with the fluid mechanics in order to accommodate for the pressure variation due to the density ratio between the phases. This is done by solving at once the hyperbolic part of the system, which include the advection, the pressure gradient and the phase change term. An ideal discretization that would strongly

couple phase change to both the heat equation and the pressure variation could be studied in future works.

The interface conditions that have been presented in Section 2 are actually never explicitly used in the code. They are implicitly contained into the global model Eq. (21). They are present in the solution in the same way as Hugoniot conditions which are never explicitly imposed at shocks in a Roe-type scheme.

5 Conclusion

In order to determine the influence of phase change in a violent separated flow problem, we had to include a model of phase change into a two-phase flow simulation. In this paper we presented the different steps of the conception of this model. At each step, modeling choices had to be made. Fig. 4 summarizes the possibilities that have been discussed in the present paper.

- | | |
|---|--|
| A) Scale of the model (Section 1) | <ul style="list-style-type: none"> • Microscopic "phase-field" thick interface • Macroscopic "DNS" scale • Macroscopic averaged field |
| B) Type of equation of state (Section 1) | <ul style="list-style-type: none"> • Distinguishable fluids (two EOS + order parameter) • Single Van der Walls-type EOS |
| C) Phase change mass flow rate (Section 2) | <ul style="list-style-type: none"> • Linear relaxation model • Equilibrium model |
| D) Inclusion in the global conservation equations (Section 3) | <ul style="list-style-type: none"> • Diffuse volumic term at the interface • Diffuse volumic term away from the interface • Captured shock-like interface with ad-hoc Riemann solution • Captured shock-like interface as an advection term |
| E) Numerical representation of the interface (Section 4) | <ul style="list-style-type: none"> • VOF-type interface without reconstruction
[Ancellin, Brosset and Ghidaglia (2018b)] • VOF-type interface with reconstruction
[Ancellin, Brosset and Ghidaglia (2019)] |
| F) Numerical scheme (Section 4) | <ul style="list-style-type: none"> • Roe-type approximate Riemann solver |

Figure 4: Summary of the modeling decisions discussed in this paper. The method in bold is the chosen one among all the discussed approaches

At each step, we tried to pick the alternative that is the most suited to our problem. Other strategies could have been chosen for other problems. The high number of possible combinations is the reason for the high diversity of phase change models in the literature. Nonetheless, the modeling decision are not totally independent, even if they have been presented in a linear fashion. For instance, we could have replaced the choice D by an

ad-hoc Riemann solver without incompatibility with the choice of two distinguishable EOS in B. However, the van-der-Walls type EOS in B might not be compatible with the use of an advection term as PDE in D.

In contrast with what have been stated for instance in Villegas et al. [[Villegas, Alis, Lepilliez et al. \(2016\)](#)], a relaxation model at the interface can be derived in a way that is compatible with the second law of thermodynamics. Many models of slow thermally-driven phase change prefer (with reason) to make the hypothesis of thermodynamical equilibrium at the interface. It can be seen as the limit case of an infinite relaxation rate. Even in this case, the relaxation model could be used as a numerical method to handle the Lagrange multiplier at the interface in equilibrium.

Two difficulties have to be handled to successfully simulate non-equilibrium interfacial phase change:

- Firstly, for a given rate of mass exchange, phase change leads to high variations of density, velocity and temperature near the interface and the code should be able to deal with them in a robust way. Density and velocity variations can be handled by the inclusion of the phase change term in the Riemann problem. For the temperature variation, considering the heat diffusion is a necessity.
- Secondly, the rate of mass exchange needs to be evaluated from the local conditions near the interface, in a way that is compatible with the Second Principle of Thermodynamics. Since we study brief and violent phenomena, we do not want to make any hypothesis of thermodynamical equilibrium at the interface. Thus, a relaxation model, where the interface return in a finite time to equilibrium, is considered.

Funding Statement: Most of the present work has been done during the PhD degree studies of the first author, with the support of GTT and the *Association Nationale de la Recherche et de la Technologie* (ANRT, France) through CIFRE contract 2013/1301.

Conflicts of Interest: The authors declare that they have no conflicts of interest to report regarding the present study.

References

- Abeyaratne, R.; Knowles, J. K.** (1991): Kinetic relations and the propagation of phase boundaries in solids. *Archive for Rational Mechanics and Analysis*, vol. 114, no. 2, pp. 119-154. DOI 10.1007/BF00375400.
- Arid, A.; Kousksou, T.; Jegadheeswaran, S.; Jamil, A.; Zeraouli, Y.** (2012): Numerical simulation of ice melting near the density inversion point under periodic thermal boundary conditions. *Fluid Dynamics and Material Processing*, vol. 8, no. 3, pp. 257-275.
- Alt, H. W.; Witterstein, G.** (2011): Distributional equation in the limit of phase transition for fluids. *Interfaces and Free Boundaries*, vol. 13, no. 4, pp. 531-554. DOI 10.4171/IFB/271.

Ancellin, M. (2017). *Sur la Modélisation Physique et Numérique du Changement de Phase Interfacial lors D'impacts de Vagues (Ph.D. Thesis)*. École Normale Supérieure Paris-Saclay.

Ancellin, M.; Brosset, L.; Ghidaglia, J. M. (2018a): A hyperbolic model of nonequilibrium phase change at a sharp liquid-vapor interface. In: Klingenberg, C., Westdickenberg, M., (eds.), *Theory, Numerics and Applications of Hyperbolic Problems I (Hyp2016)*, Springer Proceedings in Mathematics & Statistics, vol. 236, pp. 59-69. Springer, Cham. DOI 10.1007/978-3-319-91545-6_5

Ancellin, M.; Brosset, L.; Ghidaglia, J. M. (2018b): Numerical simulation of wave impacts with interfacial phase change: an isothermal averaged model. *European Journal of Mechanics-B/Fluids*, vol. 72, pp. 631-644. DOI 10.1016/j.euromechflu.2018.08.001.

Ancellin, M.; Brosset, L.; Ghidaglia, J. M. (2018c). Numerical study of phase change influence on wave impact loads in LNG tanks on floating structures. *ASME 2018 37th International Conference on Ocean, Offshore and Arctic Engineering (OMAE2018)*, Madrid, Spain, pp. V009T13A026. DOI 10.1115/OMAE2018-78643.

Ancellin, M.; Brosset, L.; Ghidaglia, J. M. (2019): Numerical simulation of wave impacts with interfacial phase change: an interface reconstruction scheme. *European Journal of Mechanics-B/Fluids*, vol. 76, pp. 352-364. DOI 10.1016/j.euromechflu.2019.03.008.

Badam, V. K.; Kumar, V.; Durst, F.; Danov, K. (2007): Experimental and theoretical investigations on interfacial temperature jumps during evaporation. *Experimental Thermal and Fluid Science*, vol. 32, no. 1, pp. 276-292. DOI 10.1016/j.expthermflusci.2007.04.006.

Baer, M.; Nunziato, J. (1986): A two-phase mixture theory for the deflagration-to-detonation transition (ddt) in reactive granular materials. *International Journal of Multiphase Flow*, vol. 12, no. 6, pp. 861-889. DOI 10.1016/0301-9322(86)90033-9.

Bedeaux, D.; Hermans, L. J. F.; Ytrehus, T. (1990): Slow evaporation and condensation. *Physica A: Statistical Mechanics and Its Applications*, vol. 169, no. 2, pp. 263-280. DOI 10.1016/0378-4371(90)90169-S.

Bedeaux, D.; Kjelstrup, S. (2004): Irreversible thermodynamics—a tool to describe phase transitions far from global equilibrium. *Chemical Engineering Science*, vol. 59, no. 1, pp. 109-118. DOI 10.1016/j.ces.2003.09.028.

Berthoud, G. (2000): Vapor explosions. *Annual Review of Fluid Mechanics*, vol. 32, no. 1, pp. 573-611. DOI 10.1146/annurev.fluid.32.1.573.

Bestion, D. (1990): The physical closure laws in the CATHARE code. *Nuclear Engineering and Design*, vol. 124, no. 3, pp. 229-245. DOI 10.1016/0029-5493(90)90294-8.

Bond, M.; Struchtrup, H. (2004): Mean evaporation and condensation coefficients based on energy dependent condensation probability. *Physical Review E*, vol. 70, no. 6, pp. 61605. DOI 10.1103/PhysRevE.70.061605.

Braeunig, J. P. (2007). *A Pure Eulerian Method with Interface Capturing for Multi-material Fluid Flows in Dimension 1, 2 and 3 (PhD Thesis)*. École Normale Supérieure de Cachan.

Chiapolino, A.; Boivin, P.; Saurel, R. (2017): A simple phase transition relaxation solver for liquid-vapor flows. *International Journal for Numerical Methods in Fluids*, vol. 83, no. 7, pp. 583-605. DOI 10.1002/flid.4282.

Dal Maso, G.; Lefloch, P.; Murat, F. (1995): Definition and weak stability of nonconservative products. *Journal de Mathématiques Pures et Appliquées*, vol. 74, no. 6, pp. 483-548.

De Lorenzo, M.; Lafon, P.; Pelanti, M. (2019): A hyperbolic phase-transition model with non-instantaneous EoS-independent relaxation procedures. *Journal of Computational Physics*, vol. 379, pp. 279-308. DOI 10.1016/j.jcp.2018.12.002.

Delhay, J. M. (1974): Jump conditions and entropy sources in two-phase systems. local instant formulation. *International Journal of Multiphase Flow*, vol. 1, no. 3, pp. 395-409. DOI 10.1016/0301-9322(74)90012-3.

Faure, S.; Ghidaglia, J. M. (2011): Violent flows in aqueous foams I: physical and numerical models. *European Journal of Mechanics-B/Fluids*, vol. 30, no. 4, pp. 341-359. DOI 10.1016/j.euromechflu.2011.03.003.

Fechter, S.; Munz, C. D.; Rohde, C.; Zeiler, C. (2017): A sharp interface method for compressible liquid-vapor flow with phase transition and surface tension. *Journal of Computational Physics*, vol. 336, pp. 347-374. DOI 10.1016/j.jcp.2017.02.001.

Ghidaglia, J. M.; Kumbaro, A.; Le Coq, G. (2001): On the numerical solution to two fluid models via a cell centered finite volume method. *European Journal of Mechanics-B/Fluids*, vol. 20, no. 6, pp. 841-867. DOI 10.1016/S0997-7546(01)01150-5.

Godlewski, E.; Seguin, N. (2006): The Riemann problem for a simple model of phase transition. *Communications in Mathematical Sciences*, vol. 4, no. 1, pp. 227-247. DOI 10.4310/CMS.2006.v4.n1.a9.

Hardt, S.; Wondra, F. (2008): Evaporation model for interfacial flows based on a continuum-field representation of the source terms. *Journal of Computational Physics*, vol. 227, no. 11, pp. 5871-5895. DOI 10.1016/j.jcp.2008.02.020.

Ishii, M.; Hibiki, T. (2011): *Thermo-Fluid Dynamics of Two-Phase Flow*. New York: Springer.

Jamet, D.; Lebaigue, O.; Coutris, N.; Delhay, J. M. (2001): The second gradient method for the direct numerical simulation of liquid-vapor flows with phase change. *Journal of Computational Physics*, vol. 169, no. 2, pp. 624-651. DOI 10.1006/jcph.2000.6692.

Juric, D.; Tryggvason, G. (1998): Computations of boiling flows. *International Journal of Multiphase Flow*, vol. 24, no. 3, pp. 387-410. DOI 10.1016/S0301-9322(97)00050-5.

Kapila, A. K.; Menikoff, R.; Bdzil, J. B.; Son, S. F.; Stewart, D. S. (2001): Two-phase modeling of deflagration-to-detonation transition in granular materials: Reduced equations. *Physics of Fluids*, vol. 13, no. 10, pp. 3002-3024. DOI 10.1063/1.1398042.

Krafcik, M.; Velasco, E. S. (2014): Beyond Clausius-Clapeyron: determining the second derivative of a first-order phase transition line. *American Journal of Physics*, vol. 82, no. 4, pp. 301-305. DOI 10.1119/1.4858403.

- Labourdette, C.; Ghidaglia, J. M.; Redford, J.; Faure, S.** (2017): Accurate state variables for fluid flow simulation using Quicksteam and Quickmethane. *European Journal of Mechanics-B/Fluids*, vol. 65, pp. 132-140. DOI 10.1016/j.euromechflu.2017.03.003.
- Le Martelot, S.; Saurel, R.; Nkonga, B.** (2014): Towards the direct numerical simulation of nucleate boiling flows. *International Journal of Multiphase Flow*, vol. 66, pp. 62-78. DOI 10.1016/j.ijmultiphaseflow.2014.06.010.
- Le Métayer, O.; Massoni, J.; Saurel, R.** (2005): Modelling evaporation fronts with reactive Riemann solvers. *Journal of Computational Physics*, vol. 205, no. 2, pp. 567-610. DOI 10.1016/j.jcp.2004.11.021.
- Le Métayer, O.; Massoni, J.; Saurel, R.** (2004): Élaboration des lois d'état d'un liquide et de sa vapeur pour les modèles d'écoulements diphasiques. *International Journal of Thermal Sciences*, vol. 43, no. 3, pp. 265-276. DOI 10.1016/j.ijthermalsci.2003.09.002.
- Martin, D.; Chaouki, H.; Robert, J. L.; Ziegler, D.; Fafard, M.** (2016): Modelling of phase change with non-constant density using XFEM and a Lagrange multiplier. *Frontiers in Heat and Mass Transfer*, vol. 7, pp. 40.
- Menikoff, R.; Plohr, B. J.** (1989): The Riemann problem for fluid flow of real materials. *Reviews of Modern Physics*, vol. 61, no. 1, pp. 75-130. DOI 10.1103/RevModPhys.61.75.
- Merkle, C.; Rohde, C.** (2007): The sharp-interface approach for fluids with phase change: riemann problems and ghost fluid techniques. *ESAIM: Mathematical Modelling and Numerical Analysis*, vol. 41, no. 6, pp. 1089-1123. DOI 10.1051/m2an:2007048.
- Perrier, V.** (2008): The Chapman-Jouguet closure for the Riemann problem with vaporization. *SIAM Journal on Applied Mathematics*, vol. 68, no. 5, pp. 1333-1359. DOI 10.1137/060650374.
- Rohde, C.; Zeiler, C.** (2015): A relaxation Riemann solver for compressible two-phase flow with phase transition and surface tension. *Applied Numerical Mathematics*, vol. 95, pp. 267-279. DOI 10.1016/j.apnum.2014.05.001.
- Sato, Y.; Ničeno, B.** (2013): A sharp-interface phase change model for a mass-conservative interface tracking method. *Journal of Computational Physics*, vol. 249, pp. 127-161. DOI 10.1016/j.jcp.2013.04.035.
- Saurel, R.; Boivin, P.; Le Métayer, O.** (2016): A general formulation for cavitating, boiling and evaporating flows. *Computers & Fluids*, vol. 128, pp. 53-64. DOI 10.1016/j.compfluid.2016.01.004.
- Saurel, R.; Petitpas, F.; Abgrall, R.** (2008): Modelling phase transition in metastable liquids: application to cavitating and flashing flows. *Journal of Fluid Mechanics*, vol. 607, pp. 313-350. DOI 10.1017/S0022112008002061.
- Schrage, R.** (1953): *A Theoretical Study of Interphase Mass Transfer*. New York: Columbia University Press.
- Simoes-Moreira, J. R.; Shepherd, J. E.** (1999): Evaporation waves in superheated dodecane. *Journal of Fluid Mechanics*, vol. 382, pp. 63-86. DOI 10.1017/S0022112098003796.

Stefan, J. (1890): Über die Theorie der Eisbildung. *Monatshefte für Mathematik und Physik*, vol. 1, no. 1, pp. 1-6. DOI 10.1007/BF01692459.

Thein, F. (2018): *Results for Two Phase Flows with Phase Transition (Ph.D. Thesis)*. Otto-von-Guericke-Universität Magdeburg.

Tryggvason, G.; Scardovelli, R.; Zaleski, S. (2011): *Direct Numerical Simulations of Gas-Liquid Multiphase Flows*. Cambridge: Cambridge University Press.

Villegas, L. R.; Alis, R.; Lepilliez, M.; Tanguy, S. (2016): A ghost fluid/level set method for boiling flows and liquid evaporation: application to the Leidenfrost effect. *Journal of Computational Physics*, vol. 316, pp. 789-813. DOI 10.1016/j.jcp.2016.04.031.

Wang, Z.; Dong, K.; Zhan, S. (2017): Numerical analysis on unsteady internal flow in an evaporating droplet. *Fluid Dynamics and Material Processing*, vol. 13, no. 4, pp. 221-234.

Welch, S. W. J.; Wilson, J. (2000): A volume of fluid-based method for fluid flows with phase change. *Journal of Computational Physics*, vol. 160, no. 2, pp. 662-682. DOI 10.1006/jcph.2000.6481.

Witterstein, G. (2010): Sharp interface limit of phase change flows. *Advances in Mathematical Sciences and Applications*, vol. 20, no. 2, pp. 585-629.

Appendix A: Hugoniot curve for phase change shock waves

In Section 2.1, we have seen that the jump conditions at a liquid-vapor interface with phase change are similar to the Rankine-Hugoniot conditions at a shock wave, or the conditions at a combustion front.

For these applications, it is common to plot in a diagram (typically (p, τ) or (p, u)) the set of states reachable from a given state through a discontinuity following the jump conditions. For the study of shocks in fluid mechanics, such a curve is called *Hugoniot curve*. In the field of combustion, it is called *Crussart curve*. A similar curve can be drawn for phase change across a sharp interface. An example of such a curve for an evaporating liquid-vapor interface has been plotted on [Fig. A1](#).

Unlike shock waves or combustion fronts, the phase change jump conditions lead to non-physical results when no heat flux is modelled. To plot [Fig. A1](#), an arbitrary heat flux of $q = J_{l \rightarrow g} \times 6 \times 10^5 \text{ Jkg}^{-1}$ has been provided to the interface.

Depending on the evaporation rate $J_{l \rightarrow g}$, the resulting vapor will have a different state (on the blue line). Here q has been chosen high enough such that the resulting vapor is on the right-hand side of the saturation curve (in gray), in the domain of stability of the gas. Due to (5), the dashed purple lines (Rayleigh lines) have a slope proportional to $J_{l \rightarrow g}^2$. At the bottom where the Rayleigh line is tangent to the Hugoniot curve, the mass flow rate $J_{l \rightarrow g}$ is maximal. This point of maximal mass flux is called Chapman-Jouguet point.

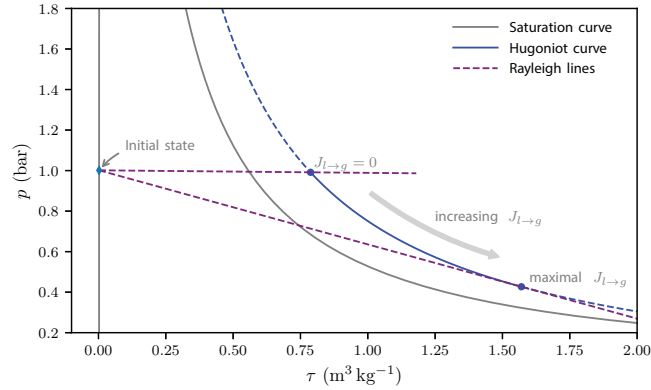


Figure A1: Hugoniot diagram for evaporation of liquid methane at $p=1$ bar and $\tau=2.3 \times 10^{-3} \text{ m}^3 \text{ kg}^{-1}$ (that is $T=111.5$ K) with a heat input of $q=J_{l \rightarrow g} \times 6 \times 10^5 \text{ J kg}^{-1}$. The equation of state used is the equation of state of methane using the tabulated *Quickmethane* [Labourdette, Ghidaglia, Redford et al. (2017)]

Appendix B: About the interpretation of non-conservative terms

In this appendix, we will briefly discuss a mathematical difficulty of the interface advection term $J \cdot \nabla \chi$. In general, the mass flow rate J should depend on the local thermodynamic state (typically p, T). However, terms of the form $J(p, T) \cdot \nabla \chi$ are not well-defined mathematically since they are the product of two distributions.

A mathematical formalism to define this kind of terms has been presented in Dal Maso et al. [Dal Maso, Lefloch and Murat (1995)]. It mainly consists in defining a smooth path between the states on both sides of the interface. For a given function $J(p, T)$ and a given regularization path, the actual mass flow rate is a function of the states on both sides of the interface $\hat{J}(p_g, T_g, p_l, T_l)$.

A physical interpretation can be seen on Fig. A2. At the beginning of this paper, we have introduced different scales of interface models: the present regularization can be interpreted as seeing the DNS scale model as the limit of a thick interface model.

Actually, in section 1 of this paper, we did not try to define an expression $J(p, T)$, but rather $J(p_g, T_g, p_l, T_l)$. In practice, we will not try to define a function $J(p, T)$, nor a regularization path: the system will be directly close by an expression of the form $J(p_g, T_g, p_l, T_l)$.

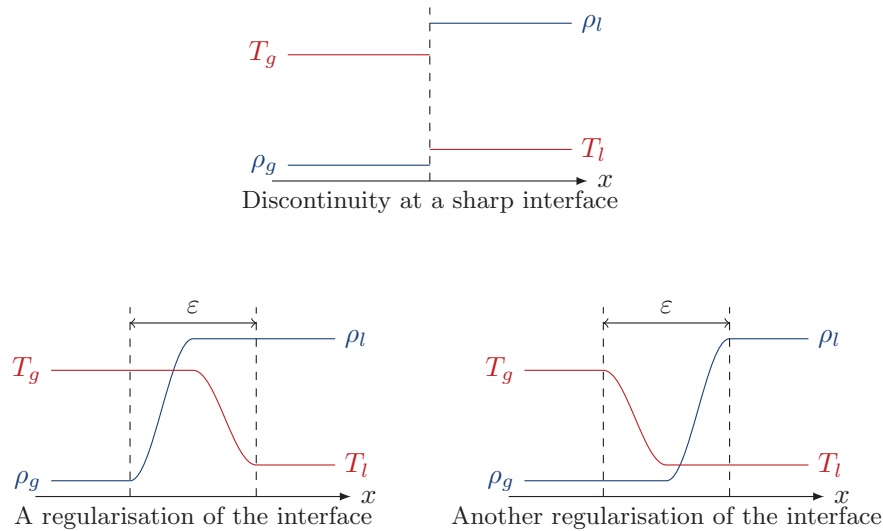


Figure A2: Two examples of regularizations (at the bottom) of a discontinuous interface (on top), or equivalently two examples of mesoscopic states (at the bottom) that are approximated by the same macroscopic model (on top). The two mesoscopic models have a different temperature at the interface (i.e., at the jump in density) and might lead to different phase change rates. Thus, the macroscopic model is in general not well-defined

Appendix C: Other shock-like models for phase change

In the present paper, only interfacial phase change has been considered. To cover more completely all possible aspects of phase change, a model should also include nucleation, that is the appearance of new interfaces (bubbles or droplets) in a pure phase. The “shock-like interface” approach can be extended to include nucleation by considering non-classical solutions to Riemann problem such as the one presented on Fig. A3 (see also e.g., [Thein (2018)]). However, the numerical simulation of nucleation at the DNS scale is difficult since it would require to track the interface of small bubble or droplets of a size smaller than the mesh.

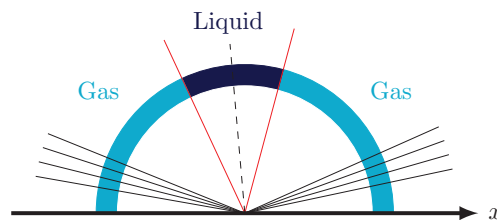


Figure A3: Riemann problem with nucleation. A liquid droplet is appearing at the center of the domain. The sudden loss of pressure in the gas is handled by the two rarefaction waves

Finally, the “phase-change shock wave” discussed in this paper are only convenient tools to represent the interface in the model and in the numerical simulation. They do not appear experimentally, since they are actually coupled with heat conduction, which is setting the pace of the process. However, when considering large-scale averaged-field models, some phase change shock waves can be observed experimentally [[Simoes-Moreira and Shepherd \(1999\)](#)]. The Riemann problem now involves a mixture of liquid and gas at equilibrium (see [Fig. A4](#)). Some of the ideas of the present paper might be useful for the numerical simulation of this phenomenon.

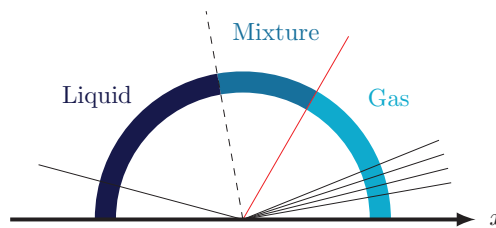


Figure A4: Multiphase mixture with partial phase change. The newly created mixture is at saturation